Frequency and Low-Temperature Characteristics of High-Q Dielectric Resonators

Y. Kobayashi, Y. Kabe, Y. Kogami, and T. Yamagishi

Department of Electrical Engineering
Saitama University
Urawa, Saitama 338, Japan

ABSTRACT

Accurate calculations of unloaded Q are described for the $TE_{01\delta}$, $TM_{01\delta}$, $EH_{11\delta}$, and $HE_{11\delta}$ modes in a dielectric rod resonator placed in a conductor cavity. These calculated results are verified experimentally. Mode designation is investigated from a viewpoint of field distribution. In particular, for high-Q $TE_{01\delta}$-mode dielectric resonators, the frequency and temperature characteristics are discussed. A typical result measured at 4 GHz shows the unloaded Q values of 45,000 at 20 °C and of 140,000 at -180 °C with the temperature coefficient of frequency of 1.5 ppm / °C.

I. INTRODUCTION

In order to construct low-loss and high-power bandpass filters we require high-Q dielectric resonators. We often use the $TE_{01\delta}$, $EH_{11\delta}$, $HE_{11\delta}$, and $TM_{01\delta}$ modes as the resonant modes. In resonator design, therefore, it is important to accurately calculate the resonant frequency f_0 and unloaded Q ,Q_u for any mode. The accurate f_0 calculation for any mode has been made from the rigorous analysis based on either radial [1] or axial [2] mode-matching technique, which is described in [3]. Only for the $TE_{01\delta}$ mode, furthermore, the Q_u value containing one due to the dielectric loss Q_d and one due to the conductor loss Q_c has been obtained accurately from the frequency calculation based on the perturbation technique [2]. For the other modes, however, we cannot use this technique for the calculating the Q_c but Q_d values.

In this paper, another technique based on calculation of stored energy and dissipated power is used for the Q calculations. The radial mode-matching technique is superior to the axial one because of no consideration for the complex modes. The calculated Q_u values must be verified by experiment to confirm the validity of the complexed calculation. The designation of the resonant modes including the hybrid modes is investigated from a viewpoint of the field distribution. Furthermore high-Q $TE_{01\delta}$-mode dielectric rod resonators are constructed from low-loss BMT ceramics developed recently. The frequency and low-temperature characteristics are discussed for these resonators.

II. ANALYSIS

Fig. 1 shows the configuration of a dielectric rod resonator analyzed. A dielectric rod resonator having the diameter D, the length L, the relative permittivity ε_r, and the loss tangent tan δ is supported with two dielectric rod having relative permittivity ε_2 ($<\varepsilon_r$) and loss tangent tan δ_2 in the center of a cylindrical conductor cavity having diameter d and height h and conductivity σ.

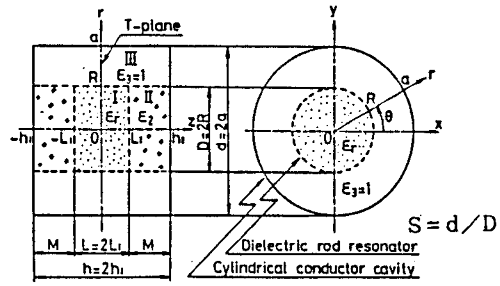

Fig. 1. Configuration of a dielectric rod resonator

For any mode of this structure, f_0 can be analyzed rigorously by the mode matching technique and calculated accurately from the following expression:

$$\det\ H(f_0, \varepsilon_r, D, L, d, h) = 0 \quad (1)$$

where elements of the determinant are given elsewhere[1]. Furthermore Q_u can be given by

$$\frac{1}{Q_u} = \frac{1}{Q_d} + \frac{1}{Q_c} = \frac{1}{Q_d} + \frac{1}{Q_{ce}} + \frac{1}{Q_{cy}} \quad (2)$$

where Q_d is due to the dielectric loss, Q_c due to the conductor loss, Q_{ce} due to the conductor plate loss, Q_{cy} due to the conductor cylinder loss. We calculate the energy stored W and the average power dissipated P in a resonator, following the definition $Q=2\pi f_0 W/P$. The details of this analysis are given elsewhere [4].

III. CALCULATION AND EXPERIMENT

Fig. 2 shows the calculated results of the resonant frequencies for some lowest modes when the distance M is increased. The resonator parameters used in this calculation are given in the figure. Considering the behavior of the resonant modes for a dielectric rod resonator with an assumed magnetic-wall cylinder,

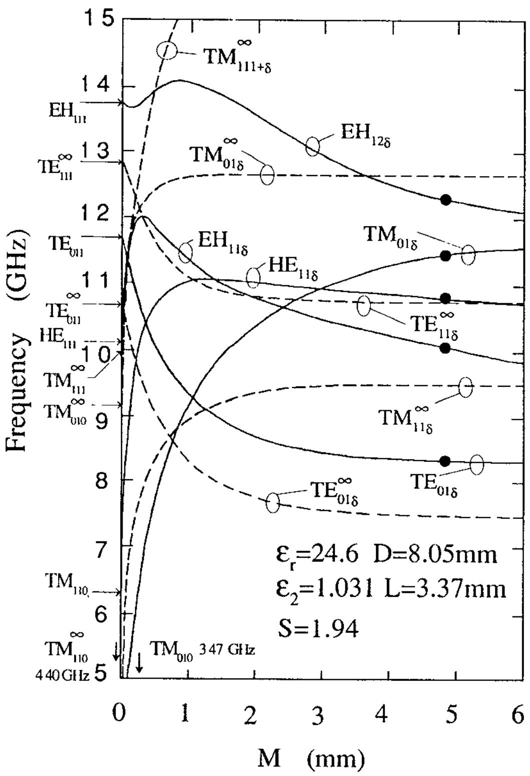

Fig. 2. The principal modes of the rod resonator
calculated
measured

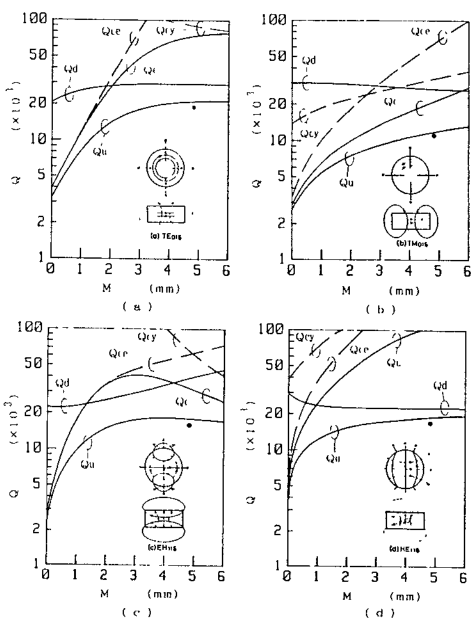

Fig. 3. The effect of M value on the Q factors.
——— calculated ● measured
D=8.05, L=3.37, s=1.9
ε_r=24.6, ε_2=1.031, tan δ=F_0(GHz)/240000, tan δ_2=4x10^{-5}
$\bar{\sigma}$ = 0.9, ($\bar{\sigma}$ =σ/σ_0 ; σ_0=58x10^6s/m)

indicated by broken lines and designated by the superscript ∞, we can expect the following mode designations when M/D≈1: (1) The TE_{011} mode at M=0 goes to the $TE_{01\delta}$ mode; (2) The TM_{010} mode to the $TM_{01\delta}$ mode; (3) The TM_{110} mode to the $HE_{11\delta}$ mode; (4) The HE_{111} mode to the $EH_{11\delta}$ mode; (5) The EH_{111} mode to the $EH_{12\delta}$ mode. The measured results of f_0 are shown in Fig. 2 by dots, which agree very well with the calculated ones.

Fig. 3 shows the results of Q_c, Q_d, and Q_u calculated for the lowest four modes in Fig. 2. The Q_c values for the $TE_{01\delta}$ mode and the Q_d values for these all modes agreed very well with the results calculated by the perturbation technique. The dots in the figures shows the measured Q_u values, which agreed with the calculated values.

IV. MODE DESIGNATION

The solid lines (a) and (b) in Fig. 4 show the results calculated for the lowest two resonant modes with

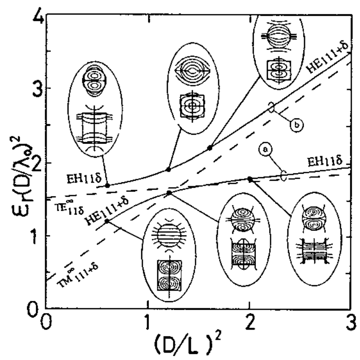

Fig. 4. The $EH_{11\delta}$ and $HE_{111+\delta}$ mode-coupling in a dielectric rod resonator and the electric field patterns.
ε_r=100, M/D=1.2, s=4
magnetic wall cylinder model for ε_r=100,M/D=∞,S=∞

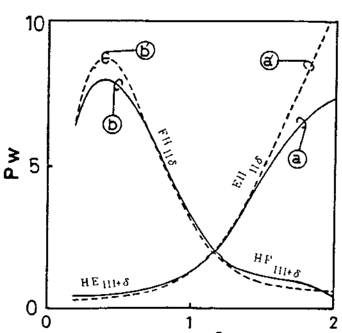

Fig. 5. Calculated P_w values for curves (a) and (b) in Fig. 4.
(a) , (b) : integration over all region in the resonator
(a'),(b') : integration over the rod only

the first subscript of 1 when $\varepsilon_r = 100$. Furthermore the electric field patterns calculated at some points on these curves are shown in this figure. The broken lines indicate the calculated results for the assumed magnetic-wall cylinder modes, the $TE^{\infty}_{11\delta}$ and $TM^{\infty}_{111+\delta}$ modes[1]. These modes do not yield mode-coupling. In contrast with this, it is found with reference to the field patterns that the coupling between the $EH_{11\delta}$ and $HE_{111+\delta}$ modes occurs when $(D/L)^2 \approx 1.2$.

Furthermore, we define P_W as $P_W=\sqrt{W^m/W^e}$, where W^m is the stored energy of the axial magnetic field component and W^e is that of the axial electric field component. Fig. 5 shows the calculated results of P_W versus $(D/L)^2$ for the curves (a) and (b) in Fig. 4. It is found from Fig. 5 that the axial magnetic field is predominant for the EH mode and the axial electric field is predominant for the HE mode. For the $EH_{nm\delta}$ and $HE_{nm\delta}$ modes, the subscript n designates the number of circumferential full wave variations of the field, the subscript m the number of radial half wave variations, and the subscript δ the number between 0 and 1 by Cohn's definition [5]. Thus, this mode designation corresponds to the convevtional mode designation for a cylindrical cavity, although this correspondence is destroied for two nomenclatures of the mode given in [2] and [3].

V. HIGH-Q $TE_{01\delta}$ MODE DIELECTRIC RESONATORS

(1) Frequency Dependence

For the $TE_{01\delta}$ mode of the resonator structure in Fig. 1, optimum dimensions to obtain the best separation from the neighboring modes [6][7] and to realize high Q_u values with appropriate separation from the neighboring modes [8] have been determined in the case of $\varepsilon_r = 24$. These two dielectric resonators, called the best-mode-separation resonator and the high-Q resonator, are compared with an TE_{011}-mode empty cavity constructed from copper-plated brass, shown in Table 1. The Q_u value of the high-Q resonator is expected to be higher than one for the empty cavity.

For the high-Q resonator and the empty cavity shown in Table 1, furthermore, the frequency dependences of Q_u were calculated when $\overline{\sigma}=1$ for copper and $f_0(THz)/\tan\delta = 200$ and 300 for low-loss BMT ceramics. These results are shown in Fig. 6. It is expected that the Q_u value for the high-Q resonator become higher than one for the empty cavity below about 10 GHz. Then the experiments were performed in the range of 4 to 50 GHz, for example Fig. 7 shows the resonator structure used in the experiment at 4 GHz. A low-loss BMT ceramic rod resonator is supported with a foamed polystyrene rod having $\varepsilon_2=1.031$ and $\tan\delta_2=4\times10^{-5}$ in a copper-plated brass cavity. Input and output excitations are performed with coupling loops. The BMT ceramics used are as follows:

(1) Ba (Zn Mg Sb Ta) O_3 (Ube Industries, Ltd.)
(2) Ba (Sn Mg Ta) O_3 (Murata Mfg. Co. Ltd.)
(3) $Ba_3 Mg Ta_2 O_9$ (Sumitomo Metal Mining Co. Ltd.)

Table 1. Comparison of $TE_{01\delta}$ dielectric rod resonators (ε_r=24) with a TE_{011} cylindrical empty cavity

	Cylindrical Empty Cavity	High Q Dielectric Resonator	Best-Mode-Separation Dielectric Resonator
Relative Volumes for Equal f_0 Values	TE_{011} Conductor	$TE_{01\delta}$ Dielectric Rod Conductor	$TE_{01\delta}$ Dielectric Rod Conductor
Cavity Volume Ratio	1	0.23	0.02
Temperature Coefficient τ_f (ppm/°C)	-20	0±1	0±1
Unloaded Q *	44000	50000	28000

* f_0 = 4 GHz, $\tan\delta = 2\cdot10^{-5}$, $\sigma = 0.9\sigma_0$, $\sigma_0 = 58\cdot10^6$ S/m

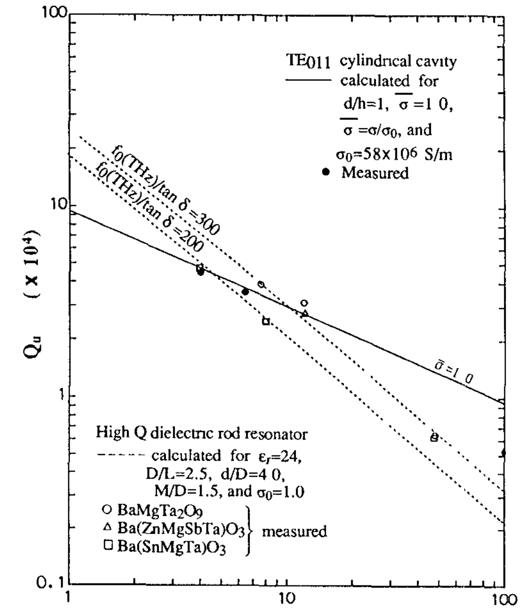

Fig. 6. Frequency characteristics of the unloaded Q, Q_u for $TE_{01\delta}$ dielectric rod resonators and a TE_{011} cylindrical cavity.

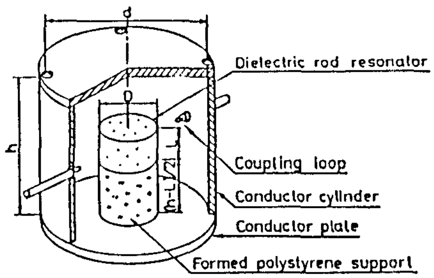

Fig. 7. Structure of a dielectric resonator placed in a cylindrical conductor cavity.

The measured Q_u values are indicated in Fig. 6 by dots. The Q_u values measured for the resonators using the material (3) are higher than ones calculated for the empty cavity. Also, the values of $f_0 / \tan\delta$ depend on the size of resonator material; that is, the $f_0 / \tan\delta$ value decreases as the material size increases.

(2) Low-Temperature Characteristics

The temperature dependences of f_0 and Q_u were measured for the high-Q resonator in Fig. 7. These results are shown in Fig. 8 by open dots. Furthermore the closed triangles in Fig. 8 indicate the Q_c values calculated using the relative resistivity $\overline{\rho} = 1/\overline{\sigma}$ in Fig. 9 and the closed dots indicate the Q_d values obtained from the relation $1/Q_d = 1/Q_u - 1/Q_c$. It is found that the

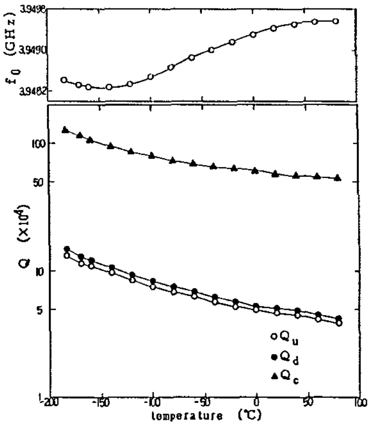

Fig. 8. Measured temperature characteristics of f_0 and Q_u for the high-Q dielectric rod resonator and calculated Q_c and Q_d values.

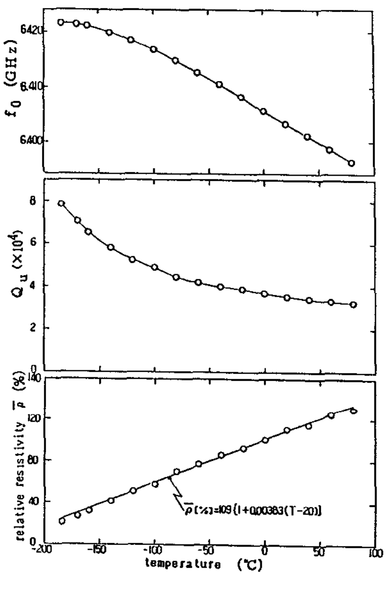

Fig. 9. Measured temperature characteristics of f_0, Q_u, and $\overline{\rho}$ for the conductor cavity.

Q_u value is determined almost by the dielectric loss. Fig. 9 shows the results for a similar measurement performed for the TE_{011} empty cavity without the dielectric rod and support. Referring to Fig. 8 and 9 we obtain the following results: (1) The temperature coefficient of f_0, τ_f is only 1.5 ppm/°C for the high Q resonator while -18 ppm/°C for the empty cavity; (2) The Q_u value of 45,000 at 20°C increases to 140,000 at -180°C for the high-Q resonator, while the Q_u value of 38,000 at 20°C increases to 78,000 at -180°C for the empty cavity. In adition, the volume of the high Q resonator is 1/4 times as well in volume as the empty cavity, as indicated in Table 1.

VI. CONCLUSIONS

Accurate Q_u calculation for any mode were performed by the rigorous analysis based on the energy estimation. The calculated Q_u values were verified by experiment. The mode designation proposed is feasible to express the field distribution.

For some high-Q $TE_{01\delta}$-mode dielectric resonators designed, the frequency and low-temperature characteristics were discussed. In comparison with conductor cavities, the excellent τ_f and Q_u characteristics as well as the small size can be realized for high-Q dielectric resonators.

ACKNOWLEDGEMENTS

The authors would like to thank M.Katoh for fabrication of resonators and T.Kobayashi for his help in numerical calculations.

REFERENCES

[1] Y. Kobayashi, N. Fukuoka, and S. Yoshida,"Resonant modes for a shielded dielectric rod resonator," Electronics and Communications in Japan, vol. 64-B, pp. 45-51, Nov. 1981.
[2] C. Chen and K. A. Zaki, "Resonant frequencies of dielectric resonators containing guided complex modes," IEEE Trans. Microwave Theory Tech., vol. MTT-36, pp.1455-1457, Oct. 1988.
[3] K. A. Michalski, "Rigorous analysis method," ch. 5 in Dielectric Resonators, D. Kaifez and P.Guillon, Ed. Dedham, MA: Artech House, 1986.
[4] Y. Kobayashi and Y. Kabe, "Analysis of unloaded Q of hybrid modes for a dielectric rod resonator," (in Japanese) Paper of Technical Group on Microwaves, IECE Japan, No. MW86-64, Oct. 1986.
[5] S. B. Cohn, "Microwave bandpass filters containing high-Q dielectric resonators, " IEEE Trans. Microwave Theory Tech., vol. MTT-16, pp. 218-227, Apr. 1968.
[6] Y. Kobayashi and M. Miura, " Optimum design of shielded dielectric rod and ring resonators for obtaining the best mode separation, " 1984 IEEE MTT-S Int. Microwave Symp. Digest, 7-11, pp.184-186.
[7] Y. Kobayashi and S. Nakayama, "Design charts for shielded dielectric rod and ring resonators," 1986 IEEE MTT-S Int. Microwave Symp. Digest, J-8, pp. 241-244.
[8] Y. Kobayashi and Y. Kabe, "Dielectric rod resonators having high values of unloaded Q," Trans. IECE Japan, vol. E 69, pp. 335-337, Apr. 1986.